

Supporting Information

Iglói et al. 10.1073/pnas.1004243107

SI Methods

Virtual Reality Design. We used a virtual reality Starmaze (1) designed with 3D StudioMax (Autodesk) and made interactive with Virtools (v3.5) (Dassault Systèmes).

Details of the Task. Before testing started, participants spent a few minutes moving freely in one alley of the environment to practice the motor aspects of the task.

For each trial, a maximal time of 90 s was allowed. If participants failed to reach the goal within 90 s, the next trial was started. The one exception was the first training trial: if participants failed to reach the goal within 90 s, they were placed in the goal alley and were told to reach the goal by going straight ahead (indicated by an arrow on the screen).

There were 48 training trials, with 16 probe trials and 16 control trials interleaved with the training trials (see Table S5 for trial order). It is important to note that participants were not informed about the existence of probe trials. During a training trial, participants were always placed in alley 1 and had to find the rewarded goal located in alley 7 (Fig. 1A). Some of the training trials (25%) ended in the middle of the goal alley with no feedback (Fig. 1A, Center).

During probe trials (Fig. 1B and C), participants had to find the goal from one of two different departure points: alley 9 for DV (different view) probe trials and alley 5 for SV (similar view) probe trials. The probe trials were designed to differentially bias the use of allocentric or sequential egocentric responses throughout the task. The view from alley 9 looked quite different from the view from the start of a training trial (compare Fig. 1A and B, Right) to make an allocentric response more likely (DV probe trial). By contrast, SV probe trials were less likely to produce an allocentric response, as the view from alley 5 (Fig. 1C, Right) was more similar to that from the start of a training trial.

During probe trials, participants did not receive any feedback: a probe trial ended when participants reached the middle of one of the goal alleys. But both strategies were considered as suitable, so a DV probe trial ended if a participant navigated to alley 7 (allocentric response) (Fig. 1B, Left) or to alley 5 (sequential egocentric response) (Fig. 1B, Center), and an SV probe trial ended if a participant navigated either to alley 7 (making an allocentric response) (Fig. 1C, Left) or to alley 1 (making a sequential egocentric response) (Fig. 1C, Center).

Control trials consisted of a navigation task in the same maze where participants had to follow a straight alley and then perform one forced turn (to the right or to the left) (Fig. 1D). All environmental features were removed to avoid encoding of landmarks (see departure view, Fig. 1D, Right) and we only made them do one body turn to avoid any sequential encoding of body turns (which could be related to a sequential egocentric strategy). As we wanted the end of the trials to correspond to a dead-end of the maze, the first alley corresponded to a central arm of the maze. This end is not distinguishable in a featureless environment from the peripheral start alley used for other trials. Participants were placed at the end of alley 5; they had to go straight ahead in the alley and turn right (into alley 4) or left (into alley 6). For every control trial, only one turn was possible; the other alley was blocked by a wall. The goal was located at the end of the final alley. The purpose of the control trial was to make subjects perform the same visuo-motor response as during normal trials, so we sought to conserve the same degree for motivation in these trials and to reward proportionally the same amount of control trials as noncontrol trials (i.e., half of the control trials ended in the middle of the goal alley with no feedback).

Behavioral Analysis. The number of visited alleys in a trial included the departure alley, all visited central and peripheral alleys (not containing the goal), and the goal alley. Distance error (DE) was the difference between the traveled path length (TPL) and the ideal path length (IPL), divided by the IPL (to allow comparison of paths with different IPLs):

$$DE(\%) = \frac{TPL - IPL}{IPL} \times 100 \quad [S1]$$

Acquisition and Analysis of Functional MRI Time Series. BOLD-sensitive T2*-weighted functional images were acquired on a 3T Siemens Allegra scanner using a gradient-echo EPI pulse sequence with the following parameters: TR = 3,120 ms, TE = 30 ms, flip angle = 90°, slice thickness = 2 mm, interslice gap = 1 mm, in-plane resolution = 3 × 3 mm, FoV = 192 mm², 48 slices per volume. The first five volumes were discarded to allow for T1 equilibration. The sequence was optimized to minimize signal dropouts in the medial temporal lobes (2). Functional images were analyzed using SPM5 (www.fil.ion.ucl.ac.uk/spm/). This analysis included standard preprocessing procedures: realignment, unwarping, slice timing to correct for differences in slice acquisition time, normalization (images were normalized to an EPI template specific to our sequence and scanner that was aligned to the MNI T1 template), and smoothing (with an isotropic 8-mm FWHM Gaussian kernel).

For all of the models, all regressors, except the movement parameters, were convolved with the SPM hemodynamic response function. Data were high-pass filtered (cut-off period = 128 s). Coefficients for each regressor were estimated for each participant by a least-mean-squares fit of the model to the time series. Linear contrasts of coefficients for each participant were entered into a second-level random-effects analysis. We report activations surviving an uncorrected statistical threshold of $P < 0.001$. Coordinates of brain regions are reported in MNI space.

For visualization of the parametric responses, we grouped trials into three to four consecutive trial groups and calculated the signal change separately for each bin (48 training trials grouped into four groups of 12 trials each, 16 control trials into four groups of 4 trials each, and allocentric or egocentric responses to probe trials separated into three groups each) (see bar plots in Fig. 4).

SI Results

Behavioral Results. A plateau in performance is reached after five training trials measured by two parameters of performance: the number of alleys (Fig. S1A, Left) and the distance error (Fig. S1A, Right). The plateau corresponds to 4.09 ± 0.26 alleys (mean \pm SEM), 4 being the minimum possible number of alleys to get to the goal (alleys 1–10, -8, -7) and $4.15 \pm 0.85\%$ virtual meters of distance error. The effect of learning is shown by a significant one way repeated-measured ANOVA with training trials as a repeated measure [$F(47, 16) = 12.91, P < 0.001$ for number of alleys, and $F(47, 16) = 16.816, P < 0.001$ for distance error]. Further Holm Sidack post hoc tests reveal no significant differences between trials from 6 to 48 ($P > 0.05$) for alleys and distance error variables, demonstrating stable performance from trial 6 on.

Debriefing Results. Out of the 16 subjects who reported having used landmarks for orientation, 14 described at least two landmark locations, 1 described the location of only one landmark, and 1 gave incorrect geographical information. Additionally, out of 17 subjects, 16 were able to draw the correct route of the training trials; 1 drew an incorrect sequence of turns.

1. Igloi K, Zaoui M, Berthoz A, Rondi-Reig L (2009) Sequential egocentric strategy is acquired as early as allocentric strategy: Parallel acquisition of these two navigation strategies. *Hippocampus* 19:1199–1211.

2. Doeller CF, King JA, Burgess N (2008) Parallel striatal and hippocampal systems for landmarks and boundaries in spatial memory. *Proc Natl Acad Sci USA* 105:5915–5920.

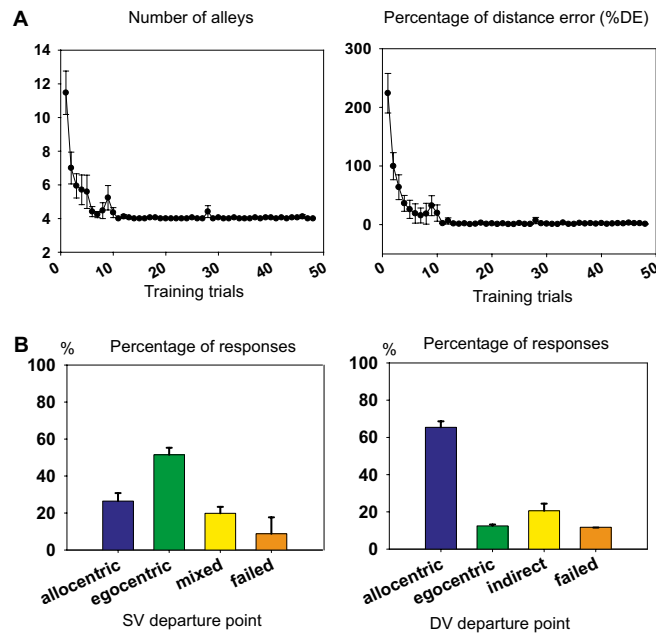


Fig. S1. Behavioral results. (A) Learning curves for training trials. (Left) Learning curve for the number of alleys visited: a plateau is reached after training trial five at 4.09 ± 0.26 alleys (mean \pm SEM). The number of alleys included departure, all visited central and peripheral alleys (not containing the goal) and the goal alley. At least four alleys are required to reach the goal (alleys 1–10, -8, -7). (Right) Learning curve for the percentage of distance error, a plateau is reached after trial five at $4.15 \pm 0.85\%$. (B) The percentage of responses made for each probe trial from the SV departure point (Left) and from the DV departure point (Right). See main text and Fig. 1 for definitions.

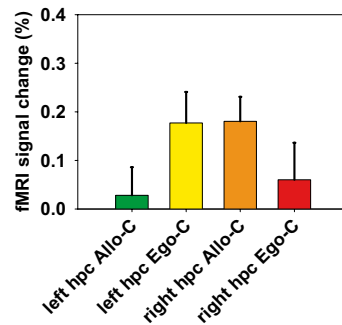


Fig. S2. Average percentage of signal change in 8-mm regions of interest in left and right hippocampus for allocentric responses versus control trials and sequential egocentric responses versus control trials, showing an interaction effect ($F = 4.4$, $P < 0.05$). Allo, allocentric; Ego, egocentric; C, control; hpc, hippocampus.

Table S1. Order of trials of the experiment

No.	Trial	No.	Trial	No.	Trial	No.	Trial
1	Training	21	Training	41	Training short	61	Training
2	Training	22	DV probe test	42	Training	62	DV probe test
3	Training	23	Training	43	DV probe test	63	Control
4	Control	24	Control	44	Control	64	Training short
5	SV probe test	25	Training short	45	Training	65	Training
6	Training short	26	Training	46	Training	66	Training short
7	Training	27	DV probe test	47	Training short	67	Training
8	Control	28	Control	48	DV probe test	68	DV probe test
9	DV probe test	29	Training	49	Training	69	Control
10	Training	30	Training short	50	Control	70	Training
11	Training short	31	Training	51	Training	71	Training short
12	Training	32	SV probe test	52	SV probe test	72	Training
13	SV probe test	33	Control	53	Control	73	SV probe test
14	Control	34	Training short	54	Training	74	Control
15	Training	35	Training	55	Training short	75	Training
16	Training	36	Training short	56	Training	76	Training
17	Training short	37	Training	57	SV probe test	77	Training short
18	SV probe test	38	SV probe test	58	Training	78	DV probe test
19	Control	39	Control	59	Control	79	Control
20	Training	40	Training	60	Training short	80	Training

Table S2. Activations for training trials vs. control trials

Area	Lat	MNI	Z score
Hippocampus	L	-21 -15 -15	3.29
Vicinity of hippocampus (extending into hippocampus)	R	30 -6 -15	5.36
Anterior cingulate	R	18 30 9	3.69
Caudate nucleus	R	18 27 0	3.02
Ventral striatum	R	12 9 -12	3.69
Vicinity of amygdala	L	-18 3 -21	3.06
Medial prefrontal cortex	L	-3 42 0	4.6
Superior frontal gyrus	L	-12 51 42	3.15
	L	-12 42 36	3
Mid-orbital gyrus	L	-3 33 -12	4.57
Insula lobe	R	42 -12 0	4.23
	L	-42 -6 -3	2.91
Rectal gyrus	L	0 42 -15	4.62
Posterior cingulate cortex	L	0 -54 30	3.56
Middle temporal gyrus	L	-54 -3 -15	2.86
	L	-63 -21 -12	2.85
	L	-42 18 -33	3.23
Precuneus	L	-12 -48 39	3.15
Cerebellum crus 2	R	27 -81 -36	4.25
	L	-45 -72 -36	3.84
	L	-33 -81 -33	2.94
Lingual gyrus	L	-6 -81 -6	4.53
	R	6 -81 -6	4.44

Table S3. Activation for allocentric and egocentric responses for probe trials vs. control trials and activations for allocentric responses vs. egocentric responses

Area	Lat	MNI	Z score	Area	Lat	MNI	Z score
Allocentric-control				Egocentric-control			
Hippocampus	R	24 -24 -9	3.71	Hippocampus	L	-21 -15 -15	3.48
Nucleus accumbens	R	12 9 -12	3.83	Anterior cingulate cortex	L	0 27 -6	4.48
	L	-12 6 -12	3.22	Nucleus accumbens	R	12 6 -15	4.36
Vicinity of caudate nucleus extending into caudate	R	18 27 0	4.13	Vicinity of caudate extending into caudate	R	21 -6 27	3.63
		18 27 9	2.87				
Anterior cingulate cortex	R	3 33 -3	3.73	Medial prefrontal cortex	L	-3 60 18	5.70
Superior frontal gyrus	L	-24 60 3	3.49	Insula lobe	R	39 -12 6	3.42
	L	-15 63 3	3.34	Insular sulcus	R	42 -21 -3	4.48
Superior temporal gyrus	R	66 -6 -9	3.72		L	-42 -21 0	3.89
Precuneus	L	3 -63 36	3.48	Rolandic operculum	R	57 -3 9	3.1
	L	-9 -57 45	3.4	Superior temporal gyrus	R	57 -18 -6	3.36
	L	6 -69 30	3.34		R	39 18 -33	3.28
Cerebellum IV-V	L	-9 -42 -12	3.72		L	-48 -33 6	3.42
Cerebellum crus 1	L	-45 -72 -36	3.28		L	-66 -36 12	3.33
Cuneus	R	12 -90 30	3.01	Middle temporal gyrus	L	-42 18 -33	3.03
	R	12 -84 39	2.84		L	-33 24 -30	2.8
Lingual gyrus	L	-6 -81 -6	5.15	Amygdala	R	30 0 -21	3.34
	L	-18 -69 -3	3.77		R	30 -6 -15	3.02
	R	6 -78 -3	4.64	Postcentral gyrus	R	21 -33 72	3.1
	R	18 -69 -3	4.33		L	-42 -15 33	2.86
Allocentric-egocentric				Precentral gyrus	R	48 -15 45	3.12
Parahippocampal gyrus	R	24 -39 -6	3.56		R	42 -15 36	3.06
Fusiform gyrus	R	33 -45 -9	3.17	Cuneus	R	9 -81 27	3.1
Parieto-occipital sulcus	R	18 -54 15	4.34	Cerebellum crus 2	R	36 -75 -39	3.12
	L	-15 -57 18	4.01		R	27 -78 -39	3.05
Inferior parietal lobule	L	-36 -57 42	3.86		R	27 -87 -36	2.77
	L	-42 -48 42	3.85	Lingual gyrus	R	6 -84 -6	4.16
Middle occipital gyrus	L	-30 -69 36	3.95	Egocentric-allocentric			
Angular gyrus	R	48 -72 30	3.89	Heschls gyrus	L	-48 -9 6	3.69
Precuneus (posterior parietal sulcus)	L	0 -75 45	3.91	Rolandic operculum	L	-51 -15 24	4.09
	L	-9 -69 48	3.84	Parietal cortex	L	-51 -33 6	3.97
Superior occipital gyrus	L	-15 -84 30	4.66	(ext into posterior insula)	L	-60 -30 18	3.85
Middle occipital gyrus	R	36 -66 30	4.36	Circular insular gyrus	R	48 -18 -3	3.96
	R	42 -66 24	3.88	Superior temporal gyrus	L	-51 -33 6	3.97
SMA	R	3 15 51	3.75	Middle temporal gyrus	L	-51 -12 -24	3.92
Middle frontal gyrus	R	39 60 0	3.42	Posterior cingulate	L	-12 -39 12	3.96
Insular lobe	L	-30 21 0	4.05	Medial prefrontal cortex	L	-3 60 18	4.15
	R	33 24 -3	3.75		R	6 57 18	4
Cerebellum VI	L	-36 -42 -33	4.42		L	-12 57 24	3.45
Cerebellum X	L	-27 -36 -39	4.14	Anterior cingulate cortex	L	-9 39 -3	3.53
Cerebellum IX	R	15 -45 -45	4.1		R	3 24 -6	3.49
Cerebellum VI	R	12 -78 -21	3.66	Inferior frontal gyrus p. orbitalis	L	-21 30 -12	3.63
Cerebellum crus 1	R	39 -66 -27	3.55	Medial orbital gyrus	R	18 30 -15	3.84
	R	39 -75 -24	3.26	Hippocampus (subthreshold)	L	-27 -15 -18	3.17
Lingual gyrus	L	-18 -75 -9	3.91				
Hippocampus (subthreshold)	R	24 -24 -6	2.0.25				

Table S4. Activations for the exponential model

Area	Lat	MNI	Z score	Area	Lat	MNI	Z score
Exponentially decreasing training model				Exponentially decreasing egocentric model			
Hippocampus	R	30 -12 -9	4.34	Hippocampus (extending into parahippocampus)	L	-21 -15 -21	3.08
Hippocampus	R	39 -21 -9	3.92	Supra marginal gyrus	R	51 -36 30	3.84
Substantia nigra		9 -21 -18	3.62		L	-51 -36 24	3.29
Pons		9 -15 -12	3.19		L	-63 -42 30	2.9
Inferior frontal gyrus	R	36 48 15	3.84	Precentral gyrus	R	36 -18 63	3.62
	R	33 12 33	3.3		R	57 -9 42	3.36
	R	45 12 39	3.26	Calcarine gyrus	R	21 -72 15	3.31
Middle frontal gyrus	L	-36 57 3	3.87	Cuneus	L	-12 -81 27	3.27
Cingulate cortex	R	6 -45 39	4.5	Exponentially increasing allocentric model			
	R	9 -36 33	4.16	Precuneus (parieto-occipital sulcus)	L	-12 -66 24	3.27
Superior temporal gyrus	L	-45 -72 21	3.46		L	-12 -66 54	3.53
	R	45 -66 27	3.94		L	-12 -54 54	3.53
Posterior cingulate cortex	L	-9 -45 21	3.82		R	12 -63 30	4.91
Fusiform gyrus	R	27 -30 -18	3.88	Superior parietal lobule	R	18 -72 51	3.19
Precuneus (parieto-occipital sulcus)	L	-6 -84 21	4.3		R	12 -78 51	3.18
	L	-15 -63 33	4.27		L	-30 -63 51	3.5
Calcarine gyrus	L	3 -69 18	4.04	Superior occipital gyrus	L	-12 -96 9	3.57
Angular gyrus	L	-36 -72 33	4.45		L	-18 -72 30	3.51
	L	-33 -54 36	4.71	Parahippocampal gyrus	R	30 -27 -18	3.83
	R	36 -57 39	3.7	Superior frontal gyrus	L	-30 3 66	3.44
	R	42 -72 39	3.17		L	-21 0 63	3.36
Inferior parietal lobule	R	48 -45 39	3.8	Red nucleus		6 -15 -6	4.3
Postcentral gyrus	R	54 -18 45	3.78	Cerebellum pyramis	R	12 -66 -30	3.94
Supra marginal gyrus	R	60 -39 39	3.65	Cerebellum III	R	12 -42 -21	3.78
	R	51 -33 36	3.4	Calcarine gyrus	L	-9 -93 0	3.38
	L	-51 -42 42	3.51		L	-9 -87 -6	3.34
Cuneus	R	9 -78 30	3.91		R	15 -96 3	3.26
				Cuneus	R	12 -93 15	3.27

Table S5. Correlation between the time series in the hippocampus and the substantia nigra for each participant

Participant	R	P	Sample size
1	0.5790	0.0000	10,176
2	0.1460	1.2700e-37	7,616
3	0.1340	2.2400e-34	8,192
4	0.2390	1.7000e-91	7,008
5	0.1710	3.9900e-49	7,280
6	0.1820	7.6900e-65	8,544
7	0.3400	1.1400e-204	7,600
8	0.3420	1.7300e-214	7,840
9	0.3200	3.8800e-171	7,184
10	0.1630	2.4500e-49	8,144
11	0.3170	1.1800e-165	7,120
12	0.3180	1.5200e-181	7,760
13	0.5410	0.0000	7,536
14	0.7900	0.0000	9,968
15	0.1870	1.1100e-61	7,712
16	0.3340	8.9900e-212	8,176
17	0.2070	4.0200e-69	7,056

Mean R = 0.312.